Korean J. Chem. Eng., 39(4), 1078-1085 (2022)
DOI: 10.1007/s11814-021-0978-y

pISSN: 0256-1115
eISSN: 1975-7220

Effect of Fe nanoparticle-loaded sawdust carbon on catalytic pyrolysis of heavy oil

Yitang Zhong*, Xiaodong Tang*,,†, Jingjing Li*, Bin He*, Zhiqi Zhang*, and Tingbing Chen***

*College of Chemistry and Chemical Engineering, Southwest Petroleum University, Chengdu, 610500, P. R. China
**State Key Laboratory of Oil and Gas Reservoir Geology and Exploitation,
Southwest Petroleum University, Chengdu, 610500, P. R. China
(*Received 16 July 2021 • Revised 25 September 2021 • Accepted 10 October 2021*)

Abstract−This work was focused on the synthesis and characterization of iron nanoparticle loaded sawdust carbon (Fe/SC) by low cost green synthesis approach and its application for catalytic pyrolysis of heavy oil. Fourier transform infrared (FT-IR), X-ray diffraction (XRD), scanning electron microscope (SEM), energy dispersive spectroscopy (EDS), transmission electron microscope (TEM), X-ray photoelectron spectroscopy (XPS) and inductively coupled plasma optical emission spectrometer (ICP-OES) methods were used to analyze the catalyst of Fe/SC. The properties of heavy oil before and after reaction were characterized by SARA analysis, FT-IR, gas chromatography-mass spectrometry (GC-MS) and thermogravimetric analysis (TGA). The experimental results showed that after pyrolytic reaction at 350 °C for 30 min with 0.1 wt% catalyst, the viscosity of heavy oil may decrease by 80.81% with a net efficiency of catalyst of 20.68%. The catalyst of Fe/SC is promising, low cost, high efficiency, highly stable and eco-friendly for catalytic upgrading and viscosity reduction of heavy oil.

Keywords: Sawdust Carbon, Iron Nanoparticles, Heavy Oil, Catalytic Pyrolysis, Viscosity Reduction

INTRODUCTION

With the increasing exploitation of global crude oil, conventional light oil resources are less and less able to meet the needs of economic development. Heavy oil reserves are abundant worldwide and which are one of the most important alternative energy sources [1,2]. However, it is difficult to extract heavy oil from underground reservoirs, because of its high viscosity, poor fluidity, and low American Petroleum Institute (API) gravity attributed to complex composition of heavy oil. Many methods of enhanced oil recovery (EOR) have been researched, which include thermal treatment [3-5], gas injection [6], chemical flooding [7,8] and microbial recovery [9,10]. Steam flooding technology is the most widely applied for improving the efficiency of heavy oil recovery. The EOR and future processing of heavy oil have been brought huge challenges owing to high viscosity and poor fluidity of heavy oil [11,12]. So, it is very important to reduce viscosity and upgrade the fluidity of heavy oil.

At present, the methods of viscosity reduction of heavy oil principally include heating, mixing light oil, mixing surfactant and catalytic methods [13,14]. Heating and mixing light oil methods are widely used in industry, and the catalytic method is the most promising method technology, because it can irreversibly change the properties and improve the quality of heavy oil. Obviously, the catalyst plays an important part in the catalytic method.

To date, many catalysts have been investigated in the catalytic chemical field and their catalytic effects on heavy oil also studied [15-17]. Generally, catalysts for viscosity reduction of heavy oil can be divided into four categories [18]: water-soluble catalysts [19], oil-soluble catalysts [20,21], dispersed catalysts [22] and mineral catalysts [23]. It is widely accepted that they have good effects on viscosity reduction and upgrading of many heavy oils in the laboratory. This might be caused by the cleavage of C-S, C-N, C-C, etc. bonds during the pyrolytic reaction of heavy oil. Transition metal nanoparticles are widely used as catalysts in many catalytic reactions [24-26]. Compared with several other catalysts, transition metal nanoparticles with plenty of active reaction sites on their surface can be used as effective heterogeneous catalysts for various organic reactions. Besides, heterogeneous nanocatalysts can be separated from the reaction system by some simple methods, which makes catalyst recycling visible. Several transition metal nanoparticles (such as Fe, Cu, Mo, Ni) are also studied on catalytic upgrading and viscosity reduction of heavy oil, which show high catalytic activity [27]. Greff found that Fe nanoparticles and Cu nanoparticles could, respectively, reduce the viscosity of heavy oil by 62% and 74% at 200 °C for 5 h after catalytic aquathermolysis reaction [28]. Hart et al. applied the catalyst of Al_2O_3-supported Ni-Mo transition metal nanoparticles to the catalytic cracking of heavy oil at 425 °C for 10 min, and the heavy oil viscosity could be reduced by 99% [29].

In this work, a carbon-based catalyst of Fe/SC was synthesized via an impregnation method followed by calcination and which was characterized. Moreover, it was applied for catalytic pyrolysis and viscosity reduction of heavy oil in the laboratory. This work aimed to obtain low-cost and high efficiency catalyst and gain insights into the potential implementation of carbon-based catalyst in the upgrading of heavy oil.

EXPERIMENT

1. Materials

The sawdust and heavy oil were obtained from a local wood-work-

†To whom correspondence should be addressed.
E-mail: txda429@163.com

Table 1. The properties of raw material

Heavy oil		Sawdust	
Viscosity (mPa·s) at 50 °C	16,000	Elemental analysis (wt%)	
Density (g/cm^3)	0.959	C	46.08
API°	13.9	H	8.27
SARA content (wt%)		O	45.31
Saturate	37.22	N	0.25
Aromatic	23.81	S	0.09
Resin	37.58	Proximate analysis (wt%)	
Asphaltene	1.38	M_{ad}	5.56
Water content (wt%)	<1	A_{ad}	2.39
Acid number (mg KOH/g)	1.73	V_{ad}	89.64
		FC_{ad}	2.41

ad: air dried

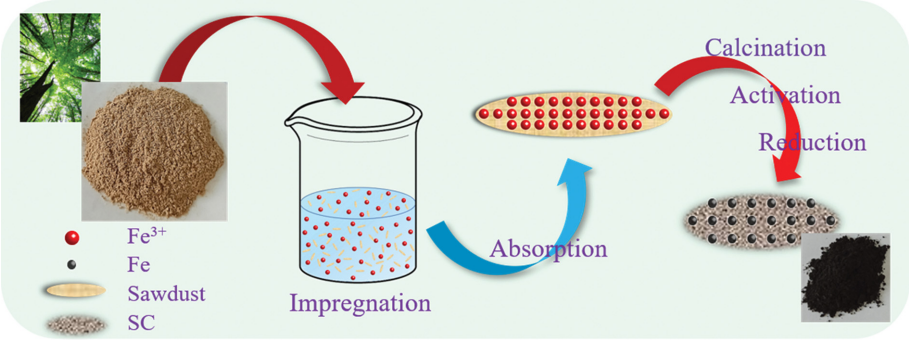

Fig. 1. Scheme of synthesis of the Fe/SC.

ing factory and Tuha oil field, Xinjiang, China, respectively. The properties of sawdust and heavy oil are shown in Table 1. Fe-PAS, an oil-soluble catalyst, was synthesized by our research group using naphthenic acid as raw material. All reagents of iron nitrate hydrate (≥98.0%), ferric chloride (≥98.0%), n-heptane (≥99.0%), tetrahydrofuran (THF, ≥99.5%), cyclohexane (CHX, 99.7%), toluene (≥99.5%), anhydrous ethanol (≥99.7%), and aluminum oxide (≥99.7%) and so on were not further processed, coming from Chengdu Kelong Chemical Reagent Co. Ltd.

2. Preparation of Catalyst

The carbon-based catalyst of Fe/SC was synthesized via an impregnation method followed by calcination at high temperature, as shown in Fig. 1. First, 2.00 g sawdust and an aqueous solution prepared by dissolving 1.30 g iron (III) nitrate hexahydrate ($Fe(NO_3)_3 \cdot 9H_2O$, AR) in 10 ml deionized water were placed into a 100 ml glass beaker. The mixture was thoroughly stirred and left at room temperature for 24 h, then dried in the oven at 80 °C for 12 h. Finally, under N_2 atmosphere, the precursor was calcined in the pipe furnace at 700 °C for 3 h; the target catalyst of Fe/SC was obtained.

3. Catalytic Upgrading Experiments

The laboratory experiments were carried out as follows. First, 90 g heavy oil, the designed amount of the powdered catalyst and hydrogen donor were put in the 500 mL autoclave. The autoclave was purged by N_2 and sealed. Then the reaction material was heated to a certain temperature and reacted for a certain time. After the reaction stopped, the temperature of reaction products dropped to about 80 °C. The gas in the autoclave was expelled, and the upgraded heavy oil sample was poured in the glass beaker for the next step analysis, which viscosity was measured with NDJ-8SN digital display viscometer (Techcomp, China). The viscosity reduction ratio (VRR) of heavy oil was calculated using the following formula:

$$VRR = \frac{\mu_0 - \mu}{\mu_0} \times 100\%$$

where μ_0 and μ are the viscosity of heavy oil samples before and after reaction, respectively.

4. Characterization

The XRD analysis of catalysts was on an X'Pert Pro diffractometer (PANalytical, The Netherlands) equipped with Cu Kα radiation at a wavelength of 0.15406 nm, operating at 40 kV and 40 mA. The morphology of the catalyst was observed with a scanning electron microscope (SEM, ZEISS EVO MA15, Germany) and a transmission electron microscope (TEM, FEI, The Netherlands). Energy-dispersive X-ray spectroscopy (EDS) analysis was carried out by a spatially resolved EDS spectroscope attached to the SEM. X-ray photoelectron spectroscopy (XPS) of the catalyst was performed by the Thermo Fisher Scientific ESCALAB 250Xi (Thermo Scientific, USA) with monochromatic Al-Kα source.

The group compositions of saturates, aromatics, resin and asphal-

tene (SARA) of heavy oil before and after reaction were separated by activated alumina chromatography column. The specific separation process was conducted according to the Standard of China Petroleum NB/SH/T 0509-2010.

FT-IR spectra of heavy oil before and after reaction were recorded employing a WQF-520 spectrometer (Beifenruili, China). The FT-IR samples were prepared with a little heavy oil about 1mg diluted to the KBr using the KBr pellet method, and the obtained spectra were normalized via OPUS 6.5 software.

Gas chromatography-mass spectrometry (GC-MS) of the saturates of oil samples was measured using the instrument (Agilent 789A-5975C, USA). The samples were obtained using n-heptane solutions containing 10 vol% of the saturates. The injector temperature was 280 °C and the spilt ratio was 10 : 1 with helium as the carrier gas. The temperature was programmed as follows: starting from 40 °C and ramped up (rate: 5 °C/min) to 280 °C. The compounds were identified by using the NIST08 and NIST08s mass spectral data library.

Thermal gravimetric analysis (TGA) of the oil samples was recorded by a Perkin-Elmer thermal analyzer (STA 8000, USA). About 10 mg of heavy oil samples was loaded into a ceramic crucible and heated from 30 °C to 800 °C at a rate of 10 °C/min.

RESULTS AND DISCUSSION

1. Characteristic Analysis of Catalyst

The XRD pattern of the prepared Fe/SC catalyst is shown in Fig. 2. Three strong diffraction peaks appear at 2θ of 44.67, 65.02, and 82.33 agreeing with the standard pattern of the cubic Fe phase (JCPDS card no. 06-0696). And a broad diffraction peak from SC centered at approximately 2θ of 25.0 can be indexed as (002) lattices. That suggests that Fe/SC composite was successfully prepared by impregnation method followed by calcination with the raw material of sawdust and $Fe(NO_3)_3{\cdot}9H_2O$. The average size of the iron nanoparticles was about 35 nm by Scherrer's formula.

The XPS spectra of the powder Fe/SC are listed in Fig. 3. From Fig. 3(a), three elements of C, O and Fe are mainly present on the sample surface. As shown in Fig. 3(b), the C1s spectra of sawdust carbon in the catalyst include the tree peaks of C-C, C-O and C=O bonds, and which correspond to the peaks at the binding energies of 284.8 eV, 285.8 eV and 288.5 eV, respectively [30]. It can be seen that the peaks at 711.0 and 707.2 eV are attributed to Fe^{3+} $2p_{3/2}$

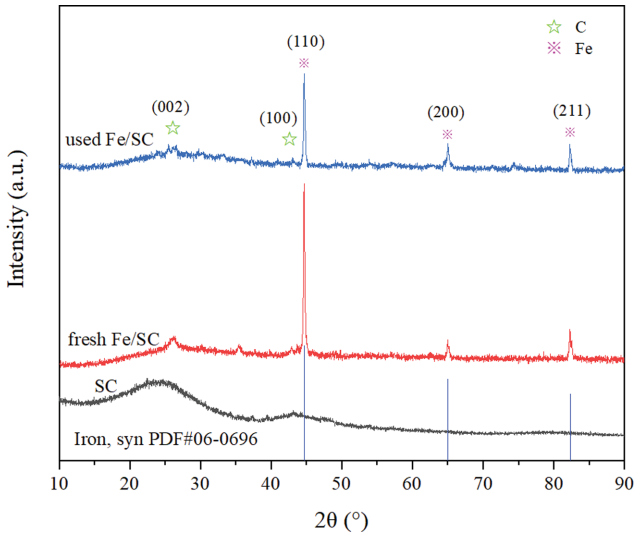

Fig. 2. XRD patterns of the fresh Fe/SC, the used Fe/SC and SC sample.

and Fe^0 $2p_{3/2}$ from the high-resolution XPS spectra of Fe 2*p* (Fig. 3(c)), respectively. The mass ratio of Fe^{3+} to Fe^0 species is 5.83 : 1 according to the XPS analysis. This further proves that the composite material of iron nanoparticles loaded sawdust carbon was synthesized successfully [31]. The Fe contents of Fe/SC as determined in the XPS and ICP-OES analysis were 16.66 wt% and 23.79 wt%, respectively. It indicates that observed uneven content of Fe in Fe/SC was because the ICP-OES technique reflected the overall composition, while XPS gave the composition at the surface.

Morphology images of the Fe/SC characterized with SEM, are shown in Fig. 4. Fig. 4(a)-(b) displays that the Fe/SC had amorphous morphology. EDS mapping was employed to further confirm the unique Fe/SC, as shown in Fig. 4(e)-(g). C and Fe elements were distributed homogeneously, which suggests that the Fe nanoparticles were dispersed uniformly on the C particles. Moreover, as shown in Fig. 2, no change in the Fe/SC catalyst before and after reaction was found by XRD except the peak intensity got a little weaker, suggesting that the Fe nanoparticles remained atomically dispersed on the SC support. It was found that there was no significant change on the effect of reusing the catalyst in Fig. S1 (Supporting Information), and the viscosity reduction ratio was more

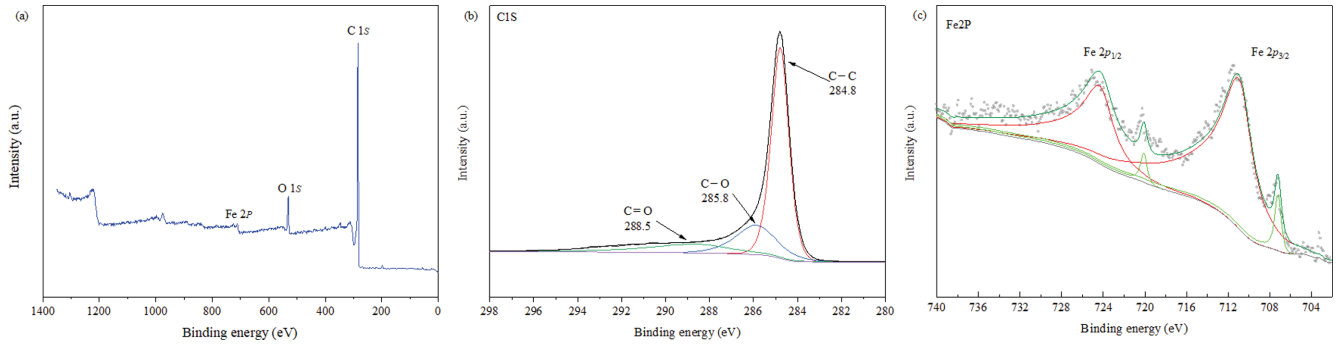

Fig. 3. XPS spectra for Fe/SC.

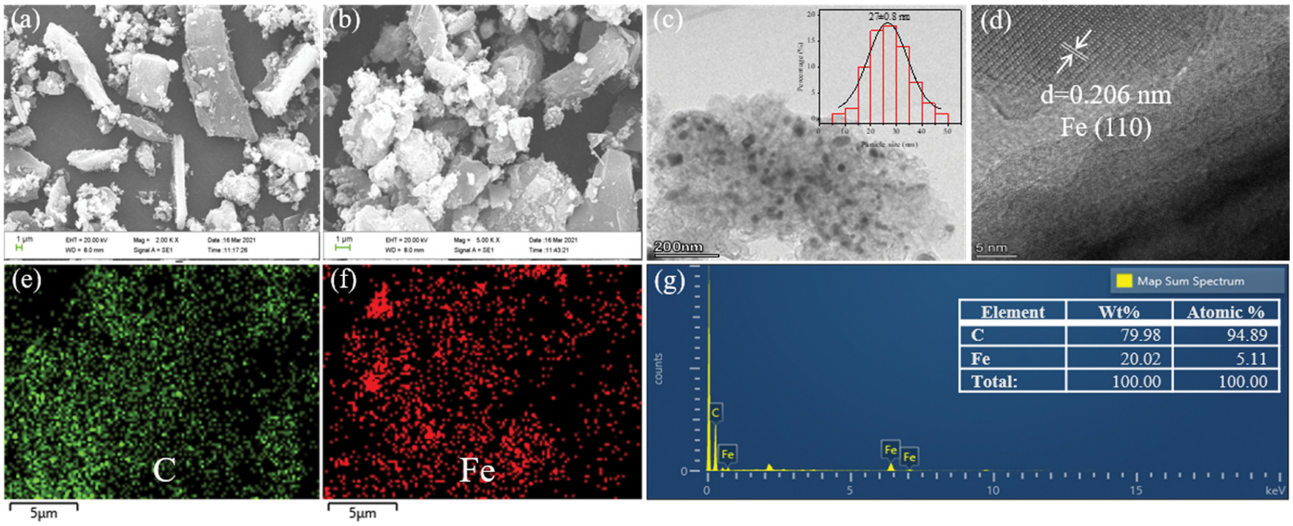

Fig. 4. (a)-(b) SEM images of Fe/SC; (c)-(d) TEM and HRTEM images of Fe/SC; (e)-(g) EDS characterization of Fe/SC of the region shown in (b).

than 79.68%, which proved that the catalyst had good stability.

TEM and high resolution (HR) TEM images of Fe/SC are shown in Fig. 4(c)-(d). It is clear that the Fe nanoparticles with an average diameter of 27 nm dispersed uniformly on the amorphous C particles, which was consistent with the SEM and the XRD results. Fig. 4(c) shows an HRTEM image of Fe/SC, and the observed lattice fringes with an interplanar spacing of 0.206 nm corresponded to the (110) lattice planes of cubic Fe, revealing that the Fe nanoparticles were crystalline.

2. Results Analysis of Catalytic Upgrading Experiment

2-1. The Effect of Catalyst Types

In this paper, the effects of dispersed catalyst of Fe/SC, oil-soluble catalyst of ferric naphthenate (Fe-PAS) and water-soluble catalyst of ferric chloride ($FeCl_3$) on upgrading and viscosity reduction of heavy oil were compared under the same reaction conditions.

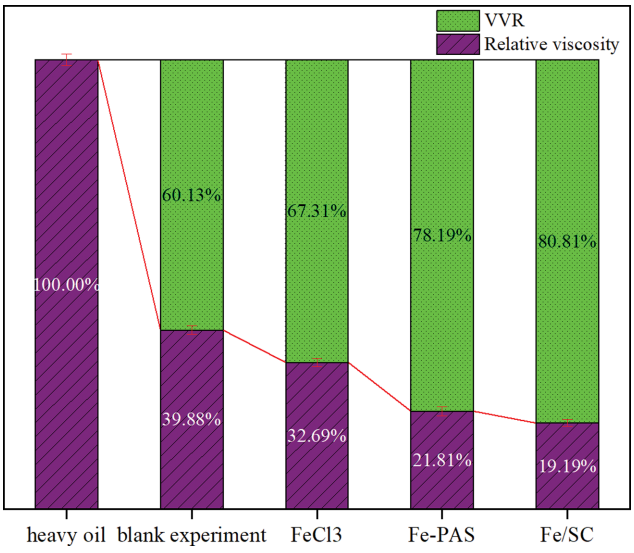

Fig. 5. Effect of different catalyst types under the same experimental condition (reaction at 350 for 30 min with 0.1 wt% catalyst).

As shown in Fig. 5, the VRR of heavy oil after reaction with a different type of catalysts was different. Among them, the effect of Fe/SC catalyst on heavy oil was almost similar to oil-soluble catalyst of Fe-PAS, but water-soluble catalyst of $FeCl_3$ was less effective than the prior two catalysts. After pyrolytic reaction with the three catalysts of Fe/SC, Fe-PAS and $FeCl_3$, the VRR of heavy oil was 80.81%, 78.19% and 67.31%, respectively. It can be seen that three different types of catalysts synthesized with the same transition metal had different effects on upgrading and viscosity reduction of heavy oil. In this work, the catalyst of Fe/SC applied in pyrolytic reaction of heavy oil was researched.

2-2. The Effect of Hydrogen Donor

Hydrogen donor had a key effect on the pyrolytic reaction of heavy oil, which could liberate hydrogen radical to impede the condensation reaction of the heavy hydrocarbon molecules during the cracking process of heavy oil. Otherwise, coke would be produced at high reaction temperature. Thus, hydrogen donor was an

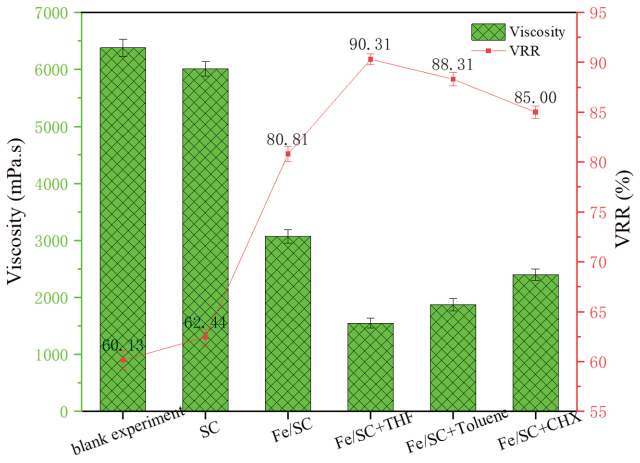

Fig. 6. Effect of different hydrogen donor under the same experimental condition (reaction at 350 for 30 min with 0.1 wt% catalyst and 3 wt% hydrogen donor).

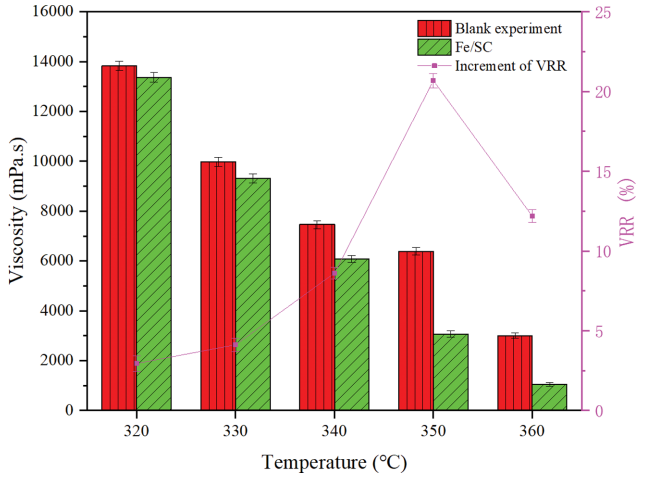

Fig. 7. Effect of reaction temperature of 320-360 °C with reaction time of 30 min and 0.1 wt% catalyst.

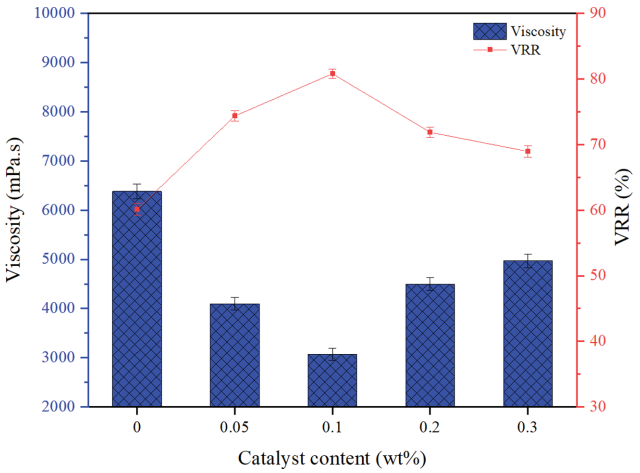

Fig. 9. Effect of the catalyst content of 0-0.3 wt% with reaction temperature of 350 °C and reaction time of 30 min.

important role in improving the quality of heavy oil.

Three different typical hydrogen donors of THF, toluene and CHX were used to participate in the pyrolytic reaction of heavy oil with the catalyst. The addition amount of hydrogen donor reagent was 3 wt%, which was selected according to the references [32,33]. The result of VVR is shown in Fig. 6 and Fig. S2. Compared to the heavy oil pyrolytic reaction with Fe/SC, there was an increment of 9.50%, 7.50% and 4.19% with the hydrogen donor addition of THF, toluene and CHX, respectively, which also suggested that the hydrogen donor had an obvious effect on catalytic pyrolytic reaction of heavy oil.

2-3. The Effect of Reaction Conditions

The viscosity reduction effect of reaction temperature, reaction time and catalyst content is shown in Figs. 7-9, respectively. From Fig. 7, compared with the pyrolytic reaction of heavy oil alone, the effects of oil samples viscosity reduction at different reaction temperatures in catalytic pyrolysis were remarkable, and the most significant viscosity reduction ratio occurred at 350 °C. Moreover, as shown in Fig. 8, with the increase of reaction time, the viscosity of oil samples first decreased rapidly and then decreased slightly, with 30 min being the optimal reaction time for the catalytic reaction of heavy oil. Finally, the influence of catalyst content on viscosity reduction of heavy oil is shown in Fig. 9. The viscosity reduction ratio of heavy oil first increased gradually and then decreased slightly with the increase of catalyst content, and the most significant effect of viscosity reduction was obtained with 0.1 wt% catalyst content. These three charts suggest that raising the reaction temperature, prolonging the reaction time and increasing catalyst content further were disadvantageous for catalytic upgrading of heavy oil, which might be due to intensified condensation phenomenon of heavy fractions during catalytic pyrolytic reaction. In conclusion, the viscosity reduction ratio of heavy oil was up to 80.81% under the optimum condition with reaction temperature of 350 °C, reaction time of 30 min and catalyst content of 0.1 wt%.

2-4. SARA Analysis

The SARA composition of heavy oil before and after pyrolytic

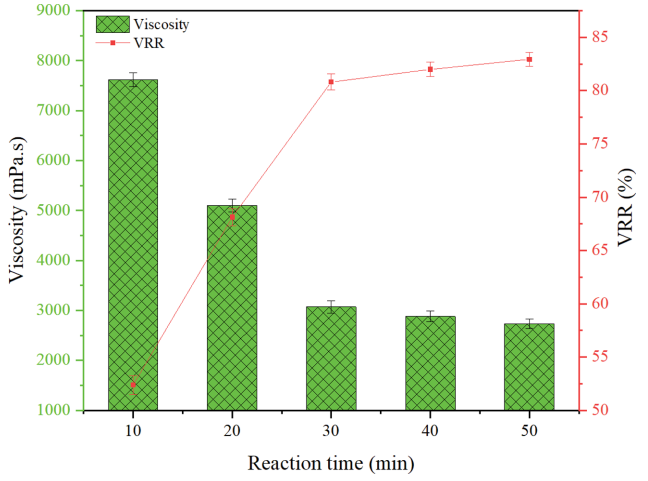

Fig. 8. Effect of reaction time of 10-50 min with reaction temperature of 350 °C and 0.1 wt% catalyst.

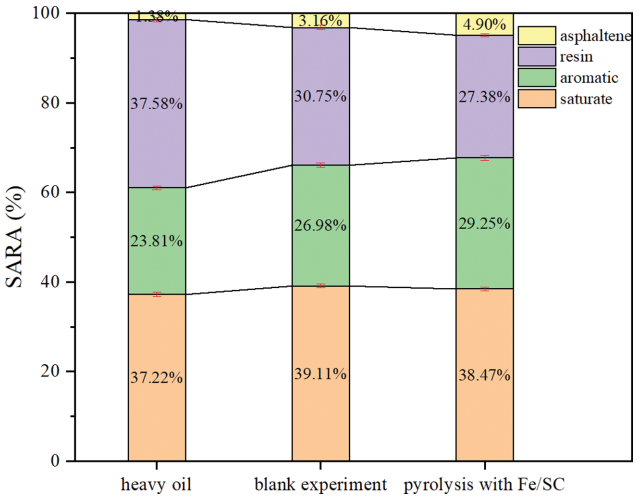

Fig. 10. SARA contents of heavy oil samples before and after reaction.

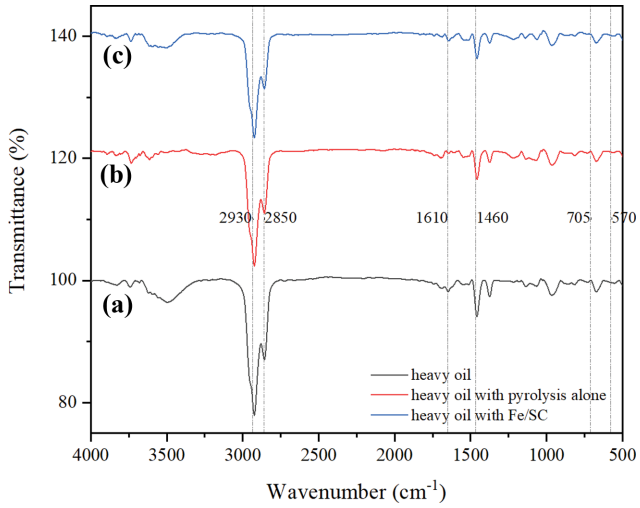

Fig. 11. FT-IR spectra of heavy oil samples before and after reaction.

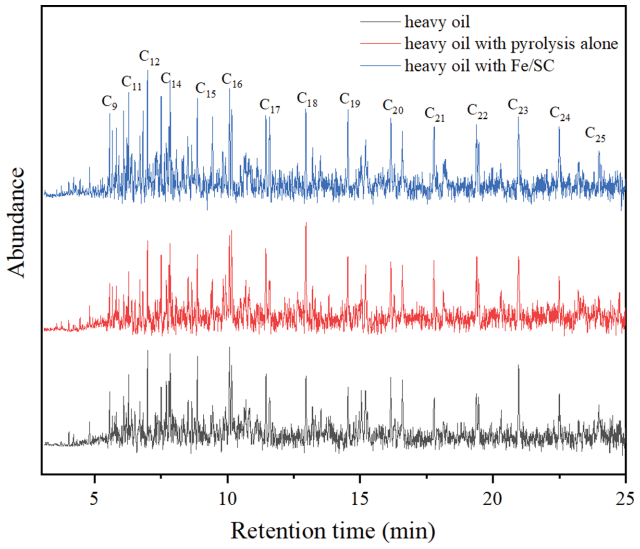

Fig. 12. GC-MS spectra of saturated hydrocarbons obtained from oil samples before and after reactions.

reaction is shown in Fig. 10. It can be seen that after pyrolytic reaction of heavy oil, the mass percentage of saturate and aromatic of light components increased, while that of resin of heavy components was reduced by 6.83%, 10.20% with pyrolysis alone and with Fe/SC catalyst, respectively. The mass percentage of asphaltene of heavy components increased slightly, which might be attributed to condensation reaction present in the pyrolytic process of heavy oil [34]. Obviously, it indicates that a part of resin was converted into other components by cracking reaction and condensation reaction, resulting in the viscosity reduction of heavy oil.

2-5. FT-IR Analysis

The variation of molecular structures was analyzed with the FT-IR spectra of oil samples, as displayed in Fig. 11. It was found that the strong absorption peaks of 2,930, 2,850 and 1,460 cm^{-1} were assigned to methyl (-CH_3) and methylene (-CH_2-). The absorption peak at 1,610 cm^{-1} was the peak of carbonyl group. The absorption peaks at 570-705 cm^{-1} referred to C-S bond [35]. From Fig. 10, the peak of methylene weakened in the heavy oil after the pyrolytic reaction, indicating that the alkyl side chains were cracked into small alkanes during the pyrolytic reaction process. Meanwhile, due to the cleavage of C-S of low bond energy, the peak of C-S weakened obviously. In brief, cleavage of long alkyl side chains and sulfur heteroatomic bridged bond contributed to enhancing the mass percentage of light compositions and reducing the mass percentage of heavy compositions, improving the quality and fluidity of heavy oil.

2-6. GC-MS Analysis

The saturated components of oil samples characterized by GC-MS before and after reaction are shown in Fig. 12. The composition of samples can be seen in Table S1 (Supporting Information). It was found that the saturated C9 to C25 in the light components of heavy oil increased significantly after pyrolytic reaction. It indicates that the saturate component was generated during catalytic pyrolysis [18]. Moreover, the quantity of saturated increased even more than that of pyrolytic reaction alone under the same reaction condition, especially C9 to C17, which also suggests that compared with pyrolysis alone, 0.1 wt% Fe/SC catalyst could further promote

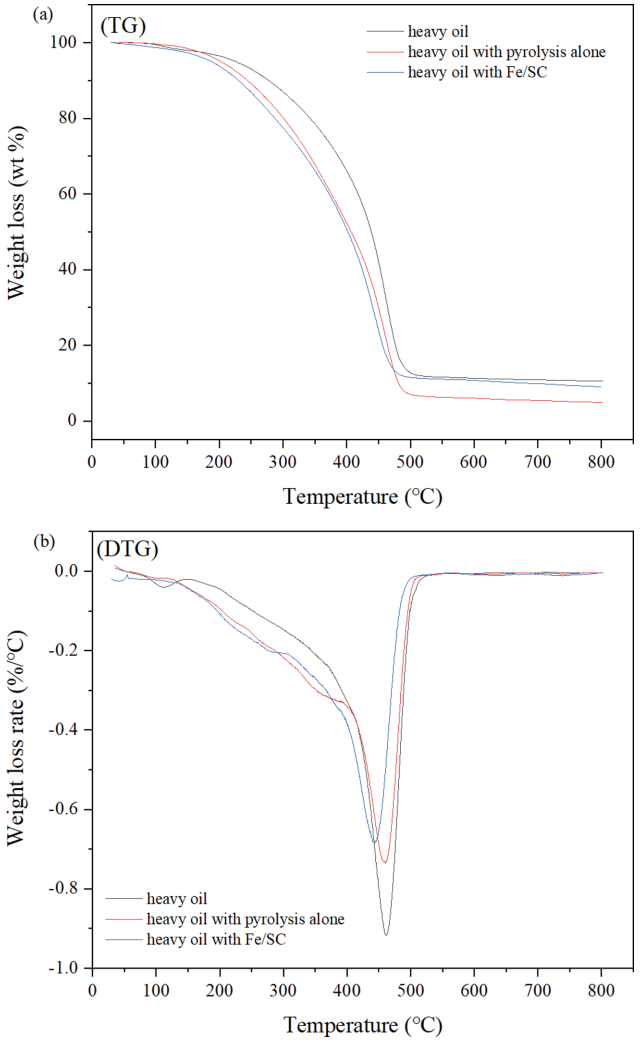

Fig. 13. TG and DTG curves of the oil samples before and after reaction.

cleavage of C-C bond. So, the catalyst of Fe/SC had an important effect on upgrading of heavy oil.

2-7. TG-DTG Analysis

Thermal decomposition of heavy oil before and after pyrolysis was studied. The TG curves of heavy oil samples at a heating rate of 10 °C/min in N_2 atmosphere are listed in Fig. 13. As shown, it can be found that the heavy oil samples had first a slight mass loss at about 100-120 °C, which might be due to moisture evaporation. Severe weight loss of the oil samples occurred in the range of 200-480 °C, which was because of the thermal decomposition as well as volatilization of feedstocks [36]. Obviously, the thermal decomposition process of different oil samples was different. Compared to thermal decomposition before reaction, the decomposition temperature of the oil samples after pyrolytic reaction with Fe/SC and with pyrolysis alone was ahead of schedule in turn, and pyrolysis degree in the 250-400 °C increased mildly, respectively. Moreover, the change trend was more distinct with Fe/SC, which indicates that Fe/SC catalyst was effective for catalytic pyrolytic reaction of heavy oil.

According to analysis and discussion of the above experimental results, it suggests that the catalyst of Fe/SC could mainly affect the cleavage of the long alkane chains, alkyl side chains and heteroatomic (thioether, etc.) bridged bonds in heavy oil chemical molecules during catalytic pyrolysis reaction. A schematic illustration of catalytic pyrolytic reaction of heavy oil is shown in Fig. 14. It is known that the active components in transition metal nanoparticles are dominative for catalytic reaction [37]. Many researchers have shown that abundant active reaction sites on Fe nanoparticles surface can reduce the apparent active energy in vast organic reaction, and which brings about the cracking of some C-C, C-N and C-S bonds during the pyrolytic reaction process of heavy oil [38]. Even the cleavage of a spot of bridge bond would distinctly improve the performance of heavy oil. In short, the catalyst can effectively promote the cracking of some chemical bonds, and it can reduce the viscosity and improve the quality of heavy oil after catalytic pyrolytic reaction. The possible catalytic pyrolysis process of heavy oil is shown in Fig. 14.

CONCLUSIONS

The catalyst of Fe/SC was successfully synthesized with $Fe(NO_3)_3 \cdot 9H_2O$ and sawdust via an impregnation method followed by calcination, which was applied to research the effect on catalytic pyrolysis of heavy oil. Analysis results of laboratory experiment indicated that the cracking degree of heavy oil significantly increased and resulted in the heavy oil viscosity decreasing obviously after catalytic pyrolysis reaction. Under the optimal reaction conditions of reaction temperature 350 °C, reaction time 30 min, catalyst content 0.1 wt%, the viscosity of heavy oil could be decreased from 16,000 mPa·s to 3,070 mPa·s with the VRR of 80.81%. The VRR of heavy oil could be further reduced by 9.50% with addition of 3.0 wt% THF after reaction. It also suggested that resin fraction and asphaltene fraction were mainly destructed to the light component during pyrolytic process of heavy oil. Compared to pyrolysis alone, the environment-friendly catalyst of Fe/SC with low cost and easy availability could increase the VRR of heavy oil by 20.68%, which is highly effective on catalytic upgrading and viscosity reduction of heavy oil.

ACKNOWLEDGEMENTS

This work was supported by the Sub topics of National Science and Technology Major Project, China (NO. 2016ZX05025-004-005).

DECLARATION OF COMPETING INTEREST

The authors declare that they have no known competing financial interests or personal relationships that could have appeared to influence the work reported in this paper.

SUPPORTING INFORMATION

Additional information as noted in the text. This information is available via the Internet at http://www.springer.com/chemistry/journal/11814.

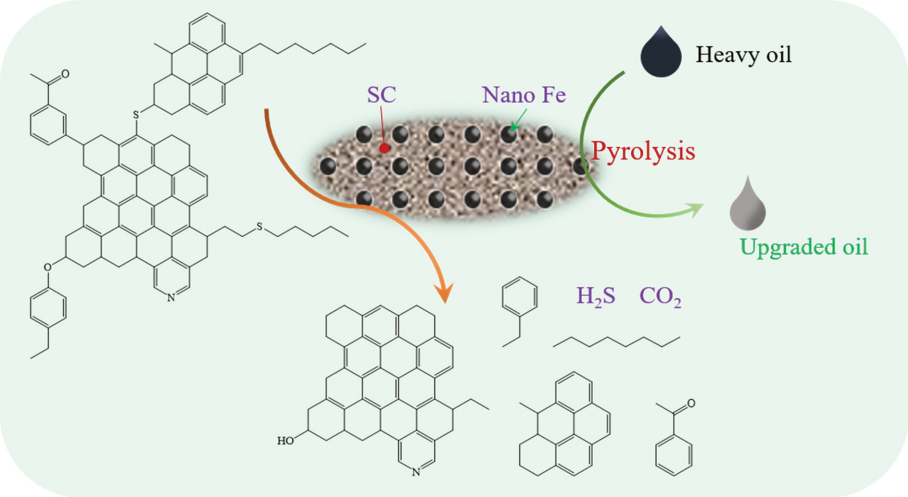

Fig. 14. Schematic illustration of catalytic pyrolysis process.

REFERENCES

1. A. Shah, R. Fishwick, J. Wood, G. Leeke, S. Rigby and M. Greaves, *Energy Environ. Sci.*, **3**, 700 (2010).
2. H. Wang, F. Ma, X. Tong, Z. Liu, X. Zhang, Z. Wu, D. Li, B. Wang, Y. Xie and L. Yang, *Petrol. Explor. Dev.*, **43**, 925 (2016).
3. Z. Pang, Y. Wu and M. Zhao, *Energy Fuels*, **30**, 2948 (2016).
4. L. Shangaraeva and V. Klimko, *Pet. Sci. Technol.*, **34**, 1894 (2016).
5. Y. Yu, Z. Chang, Y. Qi and D. Feng, *J. Pet. Explor Prod. Te.*, **8**, 947 (2017).
6. A. A. Akhmadiyarov, I. T. Rakipov, A. A. Khachatrian, A. A. Petrov, S. A. Sitnov, A. V. Gerasimov, Y. N. Osin and M. A. Varfolomeev, *J. Pet. Sci. Eng.*, **169**, 200 (2018).
7. B. Y. Jamaloei, K. Asghari and R. Kharrat, *J. Pet. Sci. Eng.*, **90-91**, 48 (2012).
8. S. L. Van and B. H. Chon, *Energies*, **9**, 711 (2016).
9. Y. B. Li, J. Wang, Y. J. Wang, D. F. Ju, Y. X. Fu, X. Y. Lei, J. Z. Jing and G. Y. Liu, *IOP Conference Series: Earth and Environmental Science*, **61**, 012137 (2017).
10. G. Wu, F. P. Ren, J. You, J. L. Yu, Y. T. Pei and S. S. Liu, *Adv. Mater. Res.*, **734-737**, 1434 (2013).
11. N. H. Abdurahman, Y. M. Rosli, N. H. Azhari and B. A. Hayder, *J. Pet. Sci. Eng.*, **90-91**, 139 (2012).
12. L. A. Strelets and S. O. Ilyin, *J. Pet. Sci. Eng.*, **203**, 108641 (2021).
13. H. A. Faris, N. A. Sami, A. A. Abdulrazak and J. S. Sangwai, *Pet. Sci. Technol.*, **33**, 952 (2015).
14. F. Homayuni, A. A. Hamidi and A. Vatani, *Pet. Sci. Technol.*, **30**, 1946 (2012).
15. Y. Chen, J. He, Y. Wang and P. Li, *Energy*, **35**, 3454 (2010).
16. F. Nakano, T. Goma, S. Suganuma, E. Tsuji and N. Katada, *Catal. Sci. Technol.*, **11**, 239 (2021).
17. Y. Wang, Y. Chen, J. He, P. Li and C. Yang, *Energy Fuels*, **24**, 1502 (2010).
18. K. Chao, Y. L. Chen, H. C. Liu, X. M. Zhang and J. Li, *Energy Fuels*, **26**, 1152 (2012).
19. L. Zhang, G. Que and W. Deng, *J. Pet. Sci. Eng.*, **73**, 27 (2010).
20. Y. Chen, Y. Wang, C. Wu and F. Xia, *Energy Fuels*, **22**, 1502 (2008).
21. Y. Xu, K. N. Heck, C. Ayala-Orozco, J. H. Arredondo, W. Zenor, M. Shammai and M. S. Wong, *Fuel*, **294**, 120546 (2021).
22. A. Al-Marshed, A. Hart, G. Leeke, M. Greaves and J. Wood, *Ind. Eng. Chem. Res.*, **54**, 10645 (2015).
23. G. P. Kayukova, A. N. Mikhailova, I. P. Kosachev, Z. R. Nasyrova, B. I. Gareev and A. V. Vakhin, *Energy Fuels*, **35**, 1297 (2021).
24. H. W. Huang, H. Zhu, Q. Zhang and C. Y. Li, *Korean J. Chem. Eng.*, **36**, 210 (2019).
25. M. Khalil, R. L. Lee and N. Liu, *Fuel*, **145**, 214 (2015).
26. M. Watanabe, H. Inomata, R. L. Smith and K. Arai, *Appl. Catal. A: Gen.*, **219**, 149 (2001).
27. C. Li, W. Huang, C. Zhou and Y. Chen, *Fuel*, **257** (2019).
28. J. Greff and T. Babadagli, *J. Pet. Sci. Eng.*, **112**, 258 (2013).
29. A. Hart, C. Lewis, T. White, M. Greaves and J. Wood, *Fuel Process. Technol.*, **138**, 724 (2015).
30. H. Viltres, O. F. Odio, L. Lartundo-Rojas and E. Reguera, *Appl. Surf. Sci.*, **511**, 145606 (2020).
31. F. S. A. Halim, S. Chandren and H. Nur, *Prog. Org. Coat.*, **147**, 105782 (2020).
32. L. O. Alemán-Vázquez, P. Torres-Mancera, J. Ancheyta and J. Ramírez-Salgado, *Energy Fuels*, **30**, 9050 (2016).
33. F. Zhao, Y. Liu, Z. Fu and X. Zhao, *Russ. J. Appl. Chem.*, **87**, 1498 (2015).
34. X.-D. Tang, T.-D. Zhou, J.-J. Li, C.-L. Deng and G.-F. Qin, *J. Anal. Appl. Pyrol.*, **143**, 104684 (2019).
35. J. Li, X. Wang, X. Tang, M. Zhang, X. Zheng, C. Wang and Z. Tang, *Fuel Process. Technol.*, **188**, 137 (2019).
36. X.-d. Tang, G.-j. Liang, J.-j. Li, Y.-t. Wei and T. Dang, *Pet. Sci. Technol.*, **35**, 1321 (2017).
37. L. Foss, N. Petrukhina, G. Kayukova, M. Amerkhanov, G. Romanov and Y. Ganeeva, *J. Pet. Sci. Eng.*, **169**, 269 (2018).
38. H. Fan, Y. Zhang and Y. Lin, *Fuel*, **83**, 2035 (2004).

Supporting Information

Effect of Fe nanoparticle-loaded sawdust carbon on catalytic pyrolysis of heavy oil

Yitang Zhong*, Xiaodong Tang*,,†, Jingjing Li*, Bin He*, Zhiqi Zhang*, and Tingbing Chen***

*College of Chemistry and Chemical Engineering, Southwest Petroleum University, Chengdu, 610500, P. R. China
**State Key Laboratory of Oil and Gas Reservoir Geology and Exploitation,
Southwest Petroleum University, Chengdu, 610500, P. R. China
(*Received 16 July 2021 • Revised 25 September 2021 • Accepted 10 October 2021*)

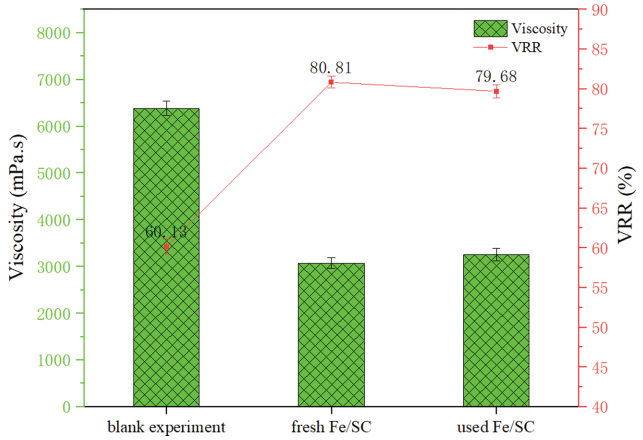

Fig. S1. Effect of the fresh and used catalyst under the same experimental condition (reaction at 350 for 30 min with 0.1 wt% catalyst).

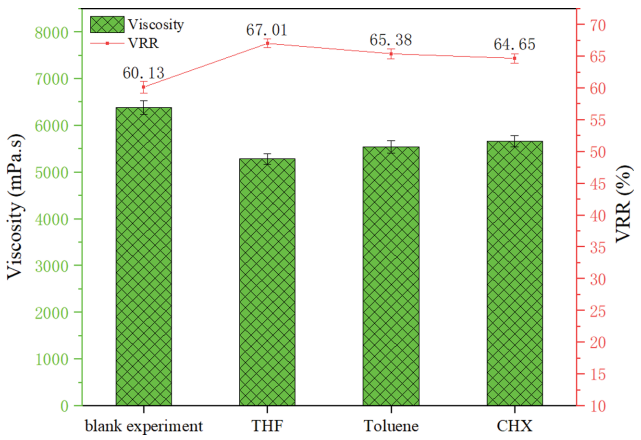

Fig. S2. Effect of different hydrogen donor without the catalyst under the same experimental condition (reaction at 350 for 30 min with 3 wt% hydrogen donor).

Table S1 The main composition of saturated hydrocarbons analyzed by GC-MS

Peak	Retention time (min)	Component		Relative content (wt%)		
				Heavy oil	Heavy oil with pyrolysis alone	Heavy oil with Fe/SC
1	5.56	C9	Nonane	0.27	0.68	1.03
2	6.28	C11	Undecane	0.43	0.66	1.05
3	6.99	C12	Dodecane	0.55	1.03	1.85
4	7.84	C14	Tetradecane	0.78	2.85	3.32
5	8.87	C15	Pentadecane	0.50	1.62	1.78
6	10.08	C16	Hexadecane	0.89	2.12	2.77
7	11.45	C17	Heptadecane	0.63	2.35	2.22
8	12.96	C18	Octadecane	0.86	3.69	2.97
9	14.54	C19	Nonadecane	0.62	2.16	2.29
10	16.16	C20	Eicosane	0.76	2.20	2.61
11	17.79	C21	Hexadecane	0.93	2.21	2.17
12	19.39	C22	Dodecane	0.89	1.89	2.47
13	20.96	C23	Tricosane	0.99	3.30	2.96
14	22.50	C24	Tetracosane	0.91	1.67	2.30
15	23.99	C25	Pentacosane	1.04	1.46	1.90
	Σ(saturated hydrocarbons)			11.05	29.89	33.69